Modelling and Multi-Variable Control of Refrigeration Systems

Larsen, Lars Finn Sloth; Holm, J. R.

Published in:
Proceedings of ECOS 2003

Publication date:
2003

Document Version
Publisher's PDF, also known as Version of record

MODELLING AND MULTI-VARIABLE CONTROL OF REFRIGERATION SYSTEMS

Lars S. Larsen and Jesper R. Holm
Central R&D - Refrigeration and Air Conditioning,
Danfoss A/S, Nordborg, Denmark

ABSTRACT

In this paper a dynamic model of a 1:1 refrigeration system is presented. The main modelling effort has been concentrated on a lumped parameter model of a shell and tube condenser. The model has shown good resemblance with experimental data from a test rig, regarding as well the static as the dynamic behavior. Based on this model the effects of the cross couplings has been examined. The influence of the cross couplings on the achievable control performance has been investigated. A MIMO controller is designed and the performance is compared with the control performance achieved by using a conventional SISO structure, which thus takes the cross couplings into account. Hereby the essential parameters that determines the magnitude of the interaction caused by the cross couplings has been clarified.

Keywords: Refrigeration systems, control schemes, modelling, shell and tube condenser.

NOMENCLATURE

A	Area $[m^2]$
c	Specific heat capacity $\left[\frac{J}{kg \cdot K}\right]$
D	Diameter $[m]$
E_c	System matrix
f_c	Vector of funtions
h	Enthalpy $\left[\frac{J}{kg}\right]$
j	Complex operator
L_c	Length of pipe i condenser $[m]$
$\dot{m}$	Mass-flow $\left[\frac{kg}{sec}\right]$
M	Molar mass $\left[\frac{kg}{mol}\right]$
n	Rot. speed of compressor $[s^{-1}]$
OD	Opening degree of valve
P	Pressure $[Pa]$
P_{sat}	Saturation pressure $[Pa]$
R	Gas constant $\left[\frac{J}{kmol \cdot K}\right]$
T	Temperature $[K]$
T_{sh}	Superheat $[K]$
T_{tw}	Temperature of water in tank $[K]$
u_c	Input vector to condenser model
V	Volume $[m^3]$
x_c	States in condenser model
α	Heat transfer coefficient $\left[\frac{W}{m^2 \cdot K}\right]$
ω	Frequency $\left[\frac{rad}{sec}\right]$
ρ	Density $\left[\frac{kg}{m^3}\right]$
$\overline{\sigma}$	Largest singular value

Subscripts

a	Ambient temperature
atc	Outer part of condenser shell
c	Condenser
ew	Evaporator wall
hw	Heating water
ic	Inlet to condenser
lc	Liquified refrigerant in condenser
oc	Outlet from condenser
sc	Pipe material in condenser
t	Condenser shell
vc	Vapor in condenser
vlc	Surface of liquid in condenser
wic	Water inlet to condenser
woc	Water outlet from condenser
woe	Water outlet from evaporator
wt	Watertank

Abbreviations

MIMO	Multi Input Multi Output
SISO	Single Input Single Output

INTRODUCTION

Refrigeration systems are widely used in applications for private consumers as well as in the industry. Despite differences in size and number of components the main construction with a valve, an evaporator, a compressor and a condenser, remains to a considerable extent the same. Great deals of the same technological challenges are therefore encountered in both markets. The subject here concerned is the efficiency of the systems. Improving the heat transfer by changing the shape of the evaporator/condenser or using extra fans on the evaporator/condenser are both ways of improving the overall efficiency. The strategy here chosen is though to utilize the potential of the evaporator to its maximum, meaning that the superheat should be kept as low as possible. This is a common control strategy used in most applications, but the improvement of variable speed compressors in the recent years has opened up for the use of more advanced control algorithms. To keep the superheat low is though not an easy task, mainly because of the non-linearities and the cross-couplings in the system. To be able to analyze the system and design high performance controllers, a system model is constructed. The model is used to design two controllers, a MIMO and a SISO, both taking the cross-couplings into considerations. These improved controllers results in a more stable superheat, meaning the level can be kept low and the efficiency improved.

SIMULATION MODEL

There are a lot of different types of refrigeration systems. The complexity of the systems, and thereby also the models, grow strongly with the number of components. Furthermore the systems normally possess a strong non-linear behavior. Because of those two characteristics it is here chosen to model a simple 1:1 refrigeration system, from which general information still can be gained. The system consists of a compressor, a condenser, an expansion valve and an evaporator as shown in Figure 1.

As load on the secondary side of the evaporator there is a flow of water coming from a 200 litre tank. The tank can be compared with a cold store room or the like with a slow dynamic. As a disturbance to the tank there is a water flow from an external reservoir. On the secondary side of the condenser a similar external water flow can be controlled manually.

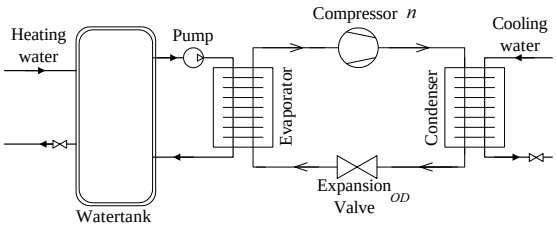

Figure 1: System layout

The four components plus the watertank are modelled separately, making it possible to validate each of them independently against experimentally data and further to replace them separately. Afterwards the components are connected to make up the whole refrigeration system. Before building the models, it has been chosen to use the rotational speed of the compressor (n) and the opening degree of the valve (OD) as input to the control, and the temperature in the watertank and the superheat as the outputs to be controlled. The compressor and the valve are modelled as static components. The equations describing the used scroll compressor are slightly modified standard equations taking the rotational speed into account, that is a 3.order polynomial fitting, where the polynomial parameters can be found as catalogue data[1]. It is assumed that the expansion valve, controlled by a stepper motor, can be modelled by the ordinary orifice equation. This means that the flow is assumed incompressible and the effects from the phase change over the valve is neglected, hereby following equation can be achieved.

$$\dot{m} \sim C_v OD \sqrt{\rho_{ref}(P_c - P_e)}, \tag{1}$$

where C_v is a constant found for the specific valve by data fitting, that among others takes the nominal opening area into account. It is assumed that the opening area is proportional with the opening degree (OD). The condenser, the evaporator and the watertank are modelled dynamically. The model structure is chosen so that ”internal” measurable process parameters can be supervised under the validation. The evaporator, being a vertical plate heat exchanger, is modelled using as a lumped parameter moving boundary model and the condenser (a shell and tube condenser) is modelled using lumped analysis and equations describing the mass and heat flow between

[1] Danfoss Compressor Catalogue and Calculation Program

the liquid- and the gas-phase. Finally the watertank is modelled using conservations of energy and the ordinary equations for heat-transfer, which results in following equation:

$$V_{wt}\rho c_p \frac{dT_{wt}}{dt} = \alpha_{wt}A_{wt}(T_a - T_{wt}) - \dot{m}_{woe}c_p(T_{wt} - T_{woe}), \quad (2)$$

In this context the density (ρ) and the specific heat capacity (c_p) both are for water.
The model of the evaporator is as mentioned based on a moving boundary model originally developed for a horizontal pipe in a cross-flow of air, which is well described in the literature [5]. When using this model certain assumptions concerning the heat transfer coefficients and mean void [4] has be to made. In order to use the model for a vertical plate heat-exchanger the lumped model of the evaporator-walls has been subjected to a slight change, because of the counter flow of water instead of the cross flow of air. This results in a altering temperature in the media on the secondary side (the water) through the evaporator. Assuming a lumped wall temperature and using conservation of energy across the walls, following partial differential equation emerge:

$$\dot{m}_{woe}c_p dT_{wt} = \alpha_{ew}A_{ew}(T_{ew} - T_w(z))dz \quad (3)$$

This equatio9ncan though easily be solved analytical and posses therefor no problem for the used numerical solver (ODE solver). The terms describing the primary side remains unchanged and can be found in [5]. The parameters in the model has been found partly form catalogue data and partly found by data fitting.
The model for the condenser seen in Figure 2, has been developed using the equations from the principles of conservation of mass, energy and volume. In the deduction the main assumptions for the condenser made are:

- The temperature of the material in the pipe and the tube are lumped parameters.
- When the refrigerant has condensed on the pipe and drops into the liquid-phase, it has reached the same temperature as the pipe.
- Each phase, liquid and the gas, are fully mixed, so that temperature distribution is uniform.

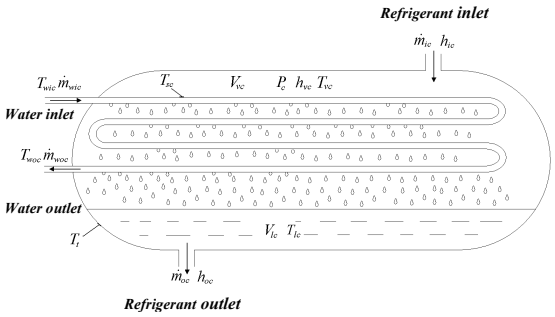

Figure 2: Shell and tube condenser

An important feature in the model is the equation for the effective mass exchange of refrigerant occurring at the surface between the liquid and the gas-phase [1]:

$$\dot{m}_{vlc} = \left(\frac{M}{2\pi R}\right)^{1/2}\left(\frac{P_c}{\sqrt{T_{vc}}} - \frac{P_{sat}(T_{lc})}{\sqrt{T_{lc}}}\right)A_{vlc}, \quad (4)$$

where $\dot{m}_{vlc}$ denotes the mass flow from the gas-phase to the liquid. This term has proven to be quite substantial and important for estimating the subcooling. By using the principles of conservation, that is:

- Conservation of mass in the gas-phase.
- Conservation of mass in the liquid-phase.
- Conservation of energy in the gas-phase.
- Conservation of energy in the liquid-phase.
- Conservation of energy in the pipe-walls.
- Conservation of energy in the condenser-tank.

The model can be deducted and written in a state space form [2]:

$$\dot{x}_c = E_c^{-1} f_c(x_c, u_c) \quad (5)$$

where

$$E_c = \begin{bmatrix} 0 & e_{12} & 0 & e_{14} & 0 & 0 \\ 0 & 0 & 0 & e_{24} & 0 & 0 \\ e_{31} & e_{32} & 0 & e_{34} & 0 & 0 \\ 0 & e_{42} & e_{43} & e_{44} & 0 & 0 \\ 0 & 0 & 0 & 0 & e_{55} & 0 \\ 0 & 0 & 0 & 0 & 0 & e_{66} \end{bmatrix}$$

$$f_c = \begin{bmatrix} \dot{m}_{ic} - \frac{\alpha_{vsc} D_{oc} \pi (T_{vc} - T_{sc}) L_c}{h_{vc} - T_{sc} c_{rc}} - \dot{m}_{vlc} \\ \frac{\alpha_{vsc} D_{oc} \pi (T_{vc} - T_{sc}) L_c}{h_{vc} - T_{sc} c_{rc}} + \dot{m}_{vlc} - \dot{m}_{oc} \\ \dot{m}_{ic} h_{ic} - \frac{\alpha_{vsc} D_{oc} \pi (T_{vc} - T_{sc}) L_c}{h_{vc} - T_{sc} c_{rc}} T_{sc} c_{rc} - \dot{m}_{vlc} h_{vc} \\ \frac{\alpha_{vsc} D_{oc} \pi (T_{vc} - T_{sc}) L_c}{h_{vc} - T_{sc} c_{rc}} T_{sc} c_{rc} + \dot{m}_{vlc} h_{vc} - \dot{m}_{oc} h_{oc} \\ \alpha_{vsc} D_{oc} \pi (T_{vc} - T_{sc}) L_c \cdots \\ -\dot{m}_{wc} c_{wc} (T_{sc} - T_{wic}) \left(1 - \exp\left(-\frac{\alpha_{vsc} D_{oc} \pi}{\dot{m}_{wc} c_{wc}} L_c\right)\right) \\ \alpha_{vtc} A_{vtc} (T_{vc} - T_t) - \alpha_{atc} A_{atc} (T_t - T_a) \end{bmatrix}$$

and

$$x_c = [h_{vc}, P_c, h_{oc}, V_{vc}, T_{sc}, T_t]^T$$

$$u_c = [\dot{m}_{ic}, h_{ic}, \dot{m}_{oc}, \dot{m}_{wc}, T_{wic}]^T$$

Expressions of the elements in E_c can be found in the appendix. It can be seen that E_c is nonsingular because of the 6 conservation equations that describes the changes in 6 states. E_c becomes singular if the condenser runs dry ($V_c = V_{vc}$), that is all the refrigerant in the condenser is in the gas-phase. In practice this means that the model is not valid when flash-gas occurs in the outlet of the condenser, meaning no subcooling.

Having build all the individual models these are connected making up the full refrigeration system, being a 12th order non-linear system (6 from the condenser 5 from the evaporator and 1 from the water-tank) with 6 inputs and two outputs. This component based way of modelling does thus introduce some algebraic constrains to the differential equations. To overcome the problems in solving these differential-algebraic equations the constrains are differentiated in order to find the underlying ordinary differential equations, which can be solved using an ordinary *MATLAB*® solver. The model is implemented in *MATLAB*® using the *NIST* refrigerant database.

In order to judge whether the model poses a satisfactorily dynamic as well as static behavior, a frequency response has been recorded on the test rig, this has been done by sending different sinus signals through the two control inputs on the test rig and afterwards evaluating the response. In Figure 3 and 4 the result has been recorded in a Bodeplot and compared to the response from the model; the model has thus previously been linearized (see next section). It should be noted, that the outputs used in this process are T_{sh} and the temperature of the water in the outlet of the evaporator (T_{woe}), which means that the tank is not included in this validation. The frequency response has been recorded at 5 different frequencies and the steady state value from a step response.

In general lies the measured response within narrow margin form the model concerning amplitude as well as phase lag, this indicates that the model at least within the measured range gives a quite good response. There is though some deviation in the response from n to T_{sh} where the model shows a resonance peak, that in practice is more dampened. Despite this deviation, it is important to notice that the amplitude of the model starts to decline at the same frequency as the recorded data and that the phase lag is correct. These are important parameters when designing a controller.

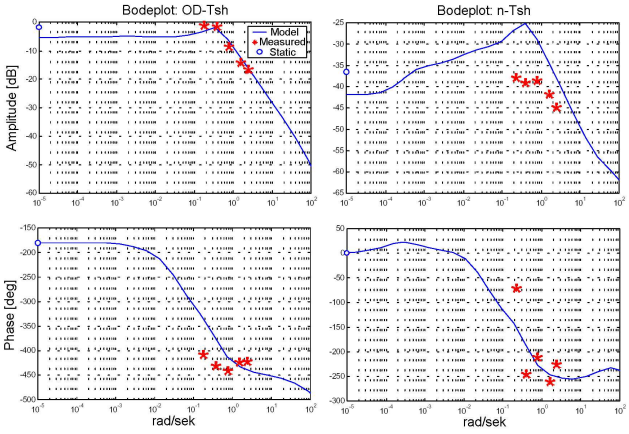

Figure 3: Bodeplot of linearized and measured transfer functions; *OD* to T_{sh} and n to T_{sh}

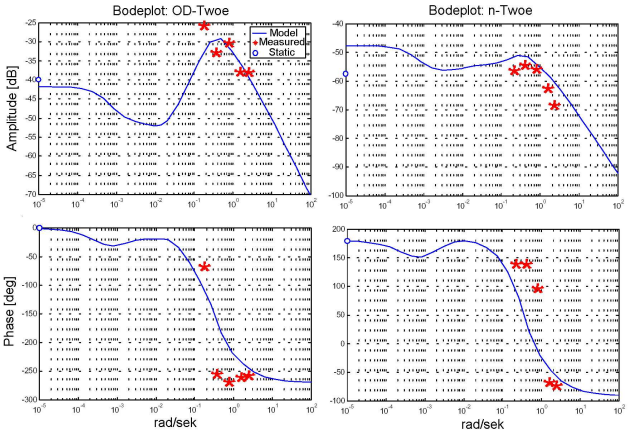

Figure 4: Bodeplot of linearized and measured transfer functions; *OD* to T_{woe} and n to T_{woe}

The model is only valid within certain limitations of which the most important are:

- That the evaporator must not be swum.

- That the condenser must not run dry.
- That the equations used for the compressor are only valid inside a working area defined by pressure and superheat plus a lower level for the rotational speed.

In practice the only actual problems encountered was a flooded evaporator and on rare occasions to low speed of the compressor.

ANALYSIS OF CROSS COUPLINGS

For a control purpose the relevant inputs to the system are the opening degree of the expansion valve (OD) and the rotational speed of the compressor (n). The normally considered outputs are the superheat (T_{sh}) and a secondary temperature, here the water temperature (T_{tw}) in the tank, see Figure 1. In most applications the expansion valve controls the superheat and the compressor the external temperature (here T_{tw}) that is two independent SISO controllers. If an abrupt change in the rotational speed of the compressor occurs, then it is common knowledge, that some interaction on the superheat will take place, even though the expansion valve controls the superheat. In other words there is an undesired cross coupling between the rotational speed of the compressor and the superheat. It is therefore useful to examine the structure of the system to determine these cross coupling, so that precautions can be taken in the controller design, whether a SISO or a MIMO controller is designed.

In order to analyze the cross couplings, the full system model is linearized using a 1.order Taylor approximation around a steady state. To derive the Taylor expansion, the Jacobians though has to be computed, which by hand is a rather considerable amount of work. Instead a numerical approximation has been used, produced by the *MATLAB*®-function "linmod". Given the following input (u) and output (y)

$$\begin{aligned} u &= \begin{bmatrix} OD \\ n \end{bmatrix} = \begin{bmatrix} 0.49 \\ 3000rpm \end{bmatrix} \\ y &= \begin{bmatrix} T_{sh} \\ T_{tw} \end{bmatrix} = \begin{bmatrix} 10.8K \\ 300.7K \end{bmatrix} \end{aligned} \tag{6}$$

and the belonging to states a transfer function matrix $G(s)$ can be found (s denotes that the system is written in the Laplace domain). Hereby the deviations from the steady state given by Eq.(6) can calculated as:

$$\begin{aligned} \Delta y(s) &= G(s)\Delta u(s) \\ \begin{bmatrix} \Delta T_{sh} \\ \Delta T_{tw} \end{bmatrix} &= \begin{bmatrix} g_{11} & g_{12} \\ g_{21} & g_{22} \end{bmatrix} \begin{bmatrix} \Delta OD \\ \Delta n \end{bmatrix}, \end{aligned} \tag{7}$$

where g_{11} is the transfer function from ΔOD to ΔT_{sh}, g_{12} is from Δn to ΔT_{sh} and so forth. By checking the steady state gain of $G(s)$ it can be determined whether it has some terms in the off-diagonal, that causes cross couplings. The steady state gain has been found to be:

$$G|_{s=0} = \begin{bmatrix} -392.83\frac{K}{OD} & 8.45\cdot 10^{-3}\frac{K}{rpm} \\ 8.11\frac{K}{OD} & -3.26\cdot 10^{-3}\frac{K}{rpm} \end{bmatrix} \tag{8}$$

This means that if OD is increased with 0.01 then at steady state the superheat will be lowered with $0.01\cdot -392.83 = -3.9K$ while the water temperature T_{tw} is increased with $0.01\cdot 8.11 = 0.08K$ and so forth. From Eq. (8) it can be seen that at least one of the off-diagonals (g_{21}) seems quite big, which at first sight indicates a strong cross coupling from OD to T_{tw}. The example showed that a small alteration in OD had a large effect on T_{sh}, though almost none on T_{tw}. Before the individual gains in G can be compared a proper scaling therefore is needed. Lets say, that we want to be able to change T_{sh} within $\pm 5K$, this means that OD should be altered $\pm\frac{5}{392.83}$. If T_{tw} should be changed within $\pm 10K$ then n should be altered $\pm\frac{10}{3.26\cdot 10^{-3}}$. By scaling G with this input range the scaled system $\widetilde{G}$ is obtained:

$$\begin{aligned} \widetilde{G} &= G|_{s=0} \begin{bmatrix} \frac{5}{392.83} & 0 \\ 0 & \frac{10}{3.26\cdot 10^{-3}} \end{bmatrix} \\ &= \begin{bmatrix} -5.00 & 25.92 \\ 0.10 & -10.00 \end{bmatrix} \end{aligned} \tag{9}$$

From this it can be seen that there is a rather large cross coupling from n to T_{sh} ($\widetilde{g}_{12}$). To give the right picture, this thus has to be evaluated against $\widetilde{g}_{11}$, because the output T_{sh} consist of contributions from as well $\widetilde{g}_{11}$ as $\widetilde{g}_{12}$. Furthermore $\widetilde{g}_{21}$ has to be evaluated against $\widetilde{g}_{22}$, therefore the system should be scaled ones more.

$$\begin{aligned} G_{scaled} &= \begin{bmatrix} \frac{1}{5} & 0 \\ 0 & \frac{1}{10} \end{bmatrix} G|_{s=0} \begin{bmatrix} \frac{5}{392.83} & 0 \\ 0 & \frac{10}{3.26\cdot 10^{-3}} \end{bmatrix} \\ &= \begin{bmatrix} -1.00 & 5.18 \\ 0.01 & -1.00 \end{bmatrix} \end{aligned} \tag{10}$$

This reveals, that the system in fact has an upper triangular structure[2], which means that T_{sh} is strongly cross coupled with n. This cross coupling should therefore be taken into consideration when the controller design is carried out.
It was assumed, that the output would stay within a certain range, which led to the chosen input scaling, which again effected the appearance of the scaled system. Not only does the size of the cross couplings in the scaled system depend on the chosen output range but on the disturbances as well. If for instance the disturbances causes T_{sh} to change a lot (more that $\pm 5K$), it would have a larger effect on T_{tw} and the term $g_{21-scaled}$ might not have been insignificant.

DESIGN OF CONTROLLERS

The foregoing analysis showed that the system indeed is cross coupled, which calls for some attention in the controller design. At first a fully cross coupled MIMO controller will be designed using the $\mathscr{H}_\infty$ design method, in order to have an optimal controller for reference. Later on this controller will be decoupled and it will be examined, which parameters in the controllers that is determinative for the interferences caused by cross couplings.
By using the $\mathscr{H}_\infty$ design method one can shape the desired closed loop transfer function towards a desired outcome. The $\mathscr{H}_\infty$-norm of a transfer function matrix ($F(s)$) is defined as the maximal gain over all frequencies [3]:

$$\|F(s)\|_\infty = \max_\omega \overline{\sigma}(F(j\omega)), \tag{11}$$

where $\overline{\sigma}$ denotes the largest singular value[3]. By using the $\mathscr{H}_\infty$ design method, the controller that minimizes the $\mathscr{H}_\infty$-norm is found. Minimizing the $\mathscr{H}_\infty$-norm causes the frequency spectra to be flatten out. If weight functions (W) are added in the output, that one wants to shape, the closed loop frequency spectra can be shaped like W^{-1}. Hereby it is possible to design a controller by choosing an appropriate setup, weight functions and a reasonable scaling of system so that performance requirements can be fulfilled, that is if the limitations of the system is not exceeded hereby.
The setup showed in Figure 5 has been used in the controller design. The weight functions has been

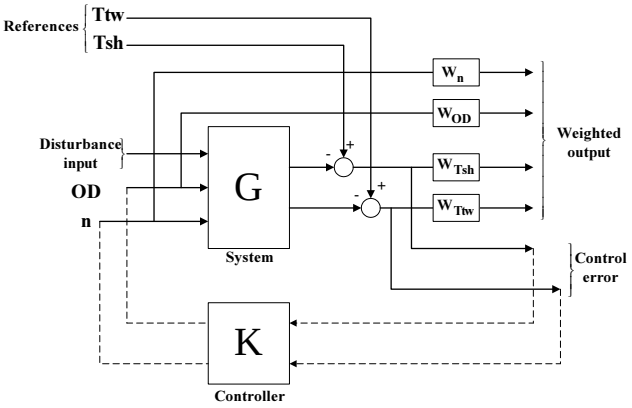

Figure 5: Setup for controller design

chosen in order to achieve a high control accuracy, rejection of disturbances and noise, suppress the cross couplings as well as to achieve robust control. A more thorough description of the selection of weight functions can be found in [2].
The $\mathscr{H}_\infty$ design method does however result in a high order controller (normally the system order plus the order of the weight functions) in other words, the controller is not practically realizable without a reduction of its order. By fitting dominating poles and zeros of the controller in the low frequency area, where control performance is needed, following reduced controller can be found:

$$K_{MIMO} = \begin{bmatrix} -0,001 \cdot \frac{35.72s+1}{35.72s} & -0,044 \cdot \frac{5000s+1}{5000s} \cdot \frac{1}{200s+1} \\ 0 & -1000 \cdot \frac{2500s+1}{2500s} \cdot \frac{1}{500s+1} \end{bmatrix} \tag{12}$$

Note that the reduced controller has the same upper triangular structure as the system has. This is due to the fact that the system only had a very weak cross coupling from n to T_{sh} (g_{21}), therefore there will be almost no loss of performance by neglecting the term, that helps suppressing the effect from the cross coupling g_{21}, namely k_{21}. Furthermore it can be seen that the terms in Eq. (12) are simple PI-controllers, thus with an "integrated" first order filter. PI-controllers are widely used and are simple to implement and tune.
Using the same setup but by lowering the demands

[2]For this kind of analysis the RGA (Λ) value is normally used, but the fact that the system has a triangular structure makes it unsuitable. $\Lambda(A) = I$ if A is a triangular matrix, which would indicate that A is a decoupled system [3].

[3]The singular value is used as a measure for the gain of a MIMO system.

on the bandwidth of the controlled output T_{tw}, the other off diagonal term in the controller can be neglected and following controller achieved [4]:

$$K_{SISO} = \begin{bmatrix} -0,001 \cdot \frac{35.72s+1}{35.72s} & 0 \\ 0 & -714 \cdot \frac{2500s+1}{2500s} \cdot \frac{1}{500s+1} \end{bmatrix} \quad (13)$$

In Figure 6 is a step response from the linearized system showed, the response has been recorded at the state around which the system was linearized given by Eq.(6). As it can be seen is the response from the

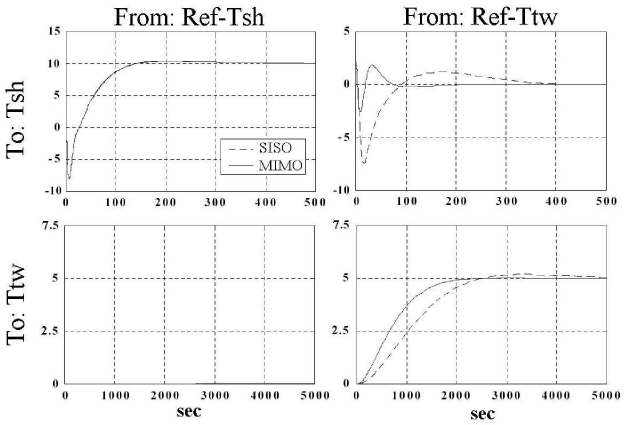

Figure 6: Step response on the linearized system model using a SISO and a MIMO controller

reference ($Ref - T_{tw}$) to T_{tw} a bit slower using the SISO controller in preference to the MIMO, which of course is a result of the lowered demand on the bandwidth. Furthermore is the interference caused by the cross coupling (cross-interaction) larger using the SISO controller, though the bandwidth of the controlled output T_{tw} in the MIMO controller is higher. As it will be shown below, plays the required bandwidth of T_{tw} an important part in the magnitude of the cross-interaction on T_{sh}, when using a SISO controller.

Using the fact that the system has an upper triangular structure and two SISO controllers' controls it, the open loop transfer function matrix can be written as:

$$GK = \begin{bmatrix} g_{11} & g_{12} \\ 0 & g_{22} \end{bmatrix} \cdot \begin{bmatrix} k_{11} & 0 \\ 0 & k_{22} \end{bmatrix} = \begin{bmatrix} g_{11}k_{11} & g_{12}k_{22} \\ 0 & g_{22}k_{22} \end{bmatrix} \quad (14)$$

The term in the off diagonal $g_{12}k_{22}$ is responsible for the cross-interaction on T_{sh}, like seen on the step response in the upper right plot in Figure 6. If though the T_{sh}-controller is faster than this "disturbance" (cross-interaction), then it will be able to suppress it. Illustrated in a Bode plot, see Figure 7, this means that $g_{11}k_{11}$ should cross the 0 dB gain (the cross over frequency) at a higher frequency than $g_{12}k_{22}$[5], that is following rule of thumb can be used:

- If $\omega_c(g_{11}k_{11}) > \omega_c(g_{12}k_{22})$ then the cross interaction on T_{sh} can be suppressed by the means of a SISO control[6].

ω_c denotes the cross over frequency, see Figure 7. Hereby it can be seen that when one wants to suppress the cross-interaction in the design of SISO control, the task is to make k_{11} large and k_{22} low, that is the bandwidth of the superheat controller (k_{11}) should be maximized whereas the bandwidth of water temperature controller (k_{22}) should be minimized. The bandwidth of k_{22} should thus still be sufficiently high to fulfill the required control performance.

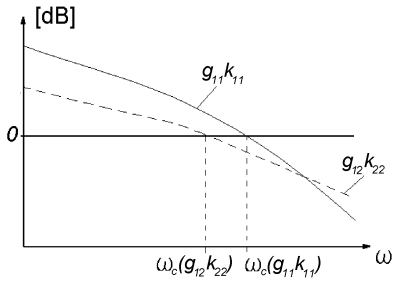

Figure 7: A sketched open loop Bode plot for a system were acceptable control can be achieved by SISO control

[4] A high bandwidth is desirable as it gives a fast response and a better rejection of disturbances

[5] At low frequencies (below the cross over frequency) control performance is needed, that is rejection of disturbances and keeping track reference changes. Beyond the cross over frequency the task is to reject noise, that is to low pass filter

[6] This only holds if $g_{11}k_{11}$ and $g_{12}k_{22}$ have nice behaviors without any resonance peaks as shown in Figure 7

Feedforward

A widely used technique to suppress the cross interaction is feedforward. By making a feedforward of the control signal from compressor n to the valve control OD, as shown in Figure 8, can the cross interaction on T_{sh} be suppressed to a great extent. Using the same notation as on Figure 8 the full con-

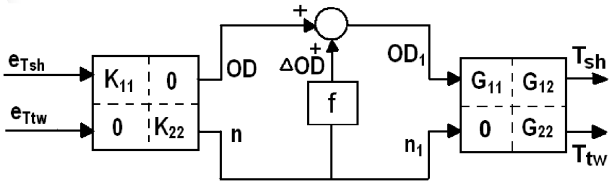

Figure 8: Feedforward of control signal from compressor.

trol can be written as:

$$\begin{bmatrix} OD_1 \\ n_1 \end{bmatrix} = \begin{bmatrix} k_{11} & 0 \\ 0 & k_{22} \end{bmatrix} \cdot \begin{bmatrix} eT_{sh} \\ eT_{tw} \end{bmatrix} + \begin{bmatrix} 0 & f \\ 0 & 0 \end{bmatrix} \cdot \begin{bmatrix} OD \\ n \end{bmatrix} \tag{15}$$

Since $n_1 = n$ and $n = k_{22} eT_{tw}$ Eq. 15 can be rewritten to:

$$\begin{bmatrix} OD_1 \\ n_1 \end{bmatrix} = \begin{bmatrix} k_{11} & f \cdot k_{22} \\ 0 & k_{22} \end{bmatrix} \cdot \begin{bmatrix} eT_{sh} \\ eT_{tw} \end{bmatrix} \tag{16}$$

Hereby it can be seen that this way of using feedforward, just is a special case of a MIMO controller.

RESULTS

The two designed controllers K_{MIMO} (12) and K_{SISO} (13) has been implemented on the test rig. They have both proven to be able to control as well the superheat T_{sh} as the water temperature T_{tw}. The main focus has though been on the cross-couplings and suppressing the effects from these in the control. Both of the controllers has been tested by making a large step in the reference on T_{tw} such that the control signal n changes rapidly in order to initiate a visible cross interaction on T_{sh}. On Figure 9 is the response on T_{sh} using these two controller shown. Note that the control signal to the compressor n saturates at 4800 RPM, why the test data cannot directly be compared to the simulation, e.g. the step response on Figure 6. As it can be seen reduces the MIMO con-

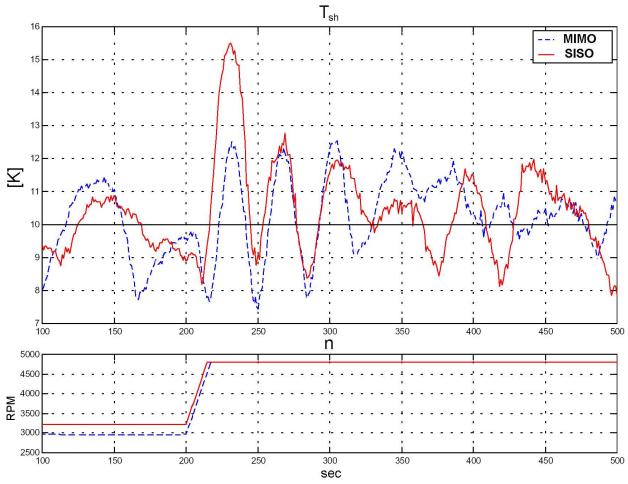

Figure 9: Cross-interaction on T_{sh} with SISO vs. MIMO control

troller the cross-interaction on T_{sh} compared to the SISO controller, though the same changes has been made on n. This reduction is however only visible when a very large bandwidth from the T_{tw}-controller (k_{22}) is required. This is in accordance to the rule of thumb stated in the controller design; the larger k_{22} compared to k_{11} the larger cross interaction.
Using either K_{SISO} or K_{MIMO} to control the system can in practise only be seen on the size of the interaction coursed by the cross-coupling. It can be seen from eq. 13 and eq. 12 that the diagonal elements almost are identical, why the step responses also are very alike except of course from the magnitude of the cross-interaction. This also appears from the simulations showed on Figure 6, for this reason only the response showing the effects from the cross-coupling has been included here.

CONCLUSIONS

A dynamic lumped parameter model of a shell and tube condenser is presented. The model takes the mass flow of refrigerant between gas- and liquid-phase into account whereby the subcooling can be described. The full model consisting of the condenser model, a dynamic moving boundary model of the evaporator and static models of the compressor and valve posed good dynamic behavior as well as static behavior.
The structural analysis revealed that the system has an upper triangular structure, that is, there is a cross coupling from the rotational speed of the compressor

to the superheat. The importance of this cross coupling though depend on the asked for output range of the superheat and the water temperature and furthermore on the magnitude of the disturbances.
By making a MIMO controller higher bandwidth of the water temperature control could be achieved, while keeping the cross interaction on the superheat to a minimum (in comparison to SISO control).
For design of SISO controllers a rule of thumb was stated, that gives a guideline to the design procedure, when the cross interaction is to be kept at a minimum.

APPENDIX

Elements in matrix E_c are:

$$e_{12} = V_{vc}\frac{\partial \rho_{vc}}{\partial P_c}$$
$$e_{14} = \rho_{vc}$$
$$e_{24} = -\rho_{lc}$$
$$e_{31} = \rho_{vc}V_{vc}$$
$$e_{32} = V_{vc}h_{vc}\frac{\partial \rho_{vc}}{\partial P_c} - V_{vc}$$
$$e_{34} = \rho_{vc}h_{vc}$$
$$e_{42} = -(V_c - V_{vc})$$
$$e_{43} = (V_c - V_{vc})\rho_{lc}$$
$$e_{44} = -\rho_{lc}h_{oc}$$
$$e_{55} = c_{sc}\rho_{sc}\pi\frac{D_{oc}^2 - D_{ic}^2}{4}L_c$$
$$e_{66} = c_t\rho_t V_t$$

REFERENCES

[1] John G. Collier. *Convective Boiling and Condensation*. McGraw-Hill, 1 edition, 1972.

[2] L. Larsen and J. Holm. Modelling and control of a refrigeration system. Master project at Technical University of Denmark, 2002.

[3] S. Skogestad and I. Postlethwaite. *Multivariable feedback control, Analysis and Design*. John Wiley & Sons, 6 edition, 2001.

[4] G. L. Wedekind, B. L. Bhatt, and B. T. Beck. A system mean void fraction model for predicting various transient phenomena associated with two-phase evaporating and condensing flows. *Int. J. Multiphase flow*, 4:97–114, 1978.

[5] H. Xiang-Dong, Sheng Liu, and H. H. Asada. Modelling of vapor compression cycles for multivariable feedback control of hvac systems. *Journal of Dynamic Systems, Measurement and Control*, 119:183–183, 1997.